Presented at the 35th European PV Solar Energy Conference and Exhibition, 24-28 September 2018, Brussels, Belgium

PRINTED DOPANT SOURCES FOR LOCALLY-DOPED SIOX/POLY-SI PASSIVATING CONTACTS

Z. Kiaee, C. Reichel, F. Feldmann, M. Jahn, J. D. Huyeng, R. Keding, M. Hermle, F. Clement
Fraunhofer Institute for Solar Energy Systems (ISE), Heidenhofstr. 2, 79110 Freiburg, Germany
Phone: +49 761 - 4588 5654; e-mail: zohreh.kiaee@ise.fraunhofer.de

ABSTRACT: This paper presents an industrially relevant solution for the formation of local passivating contacts for back-contact back-junction (BC-BJ) solar cells, based on inkjet- and screen-printing of dopant inks and pastes. The successful realization of passivating contacts utilizing printing technologies is a crucial prerequisite to simplify the fabrication process of BC-BJ cells while approaching theoretical efficiency limit of silicon solar cells. In this work, dopant inks and pastes as well as the printing parameters are tuned in order to establish a high passivation quality within c-Si/SiO_x/poly-Si lifetime samples. The impact of the anneal/diffusion conditions on the surface passivation are studied. Excellent passivation quality is achieved for inkjet-printed *n*-type (phosphorus) poly-Si surfaces with implied open-circuit voltage iV_{OC} of 726 mV and implied fill factor i*FF* of 86.2%. On *p*-type, iV_{OC} of 692 mV and i*FF* of 82.8% and iV_{OC} of 700 mV and i*FF* of 82.4% where measured by utilizing inkjet and screen-printing, respectively. Similar results were realized by Ion-implanted surfaces, herein used as the reference, underlining the high potential of the investigated printing processes.

Keywords: Inkjet, Screen-printing, Passivating contacts, BC-BJ, TOPCon

1 INTRODUCTION

One of the last remaining obstacles to approach the theoretical efficiency limit of silicon solar cells are passivating contacts [1]. Up to now, increasing the efficiency by improving the bulk lifetime and the dielectric surface passivation of silicon wafers has been extensively studied. Thus, in order to realize solar cells with efficiencies approaching the theoretical limit of 29%, passivating contacts are crucial to be developed and practically implemented in photovoltaic devices [2].

Recently, silicon solar cells with tunnel oxide passivated carrier-selective contact (TOPCon) structure [3-10] have demonstrated the great potential and received significant attention. For these types of solar cells, an ultra-thin oxide layer is implemented between polycrystalline silicon (poly-Si) and the crystalline silicon (c-Si) to deliver interface passivation of high quality. Efficiently doped poly-Si layers are used to maintain the quasi-fermi level separation in c-Si (high V_{OC}), and fulfill an efficient majority carrier transport (high *FF*).

As a result, the photo conversion efficiency of TOPCon solar cells has been continuously improved to 25.8% [11, 12], one of the highest efficiencies for crystalline silicon solar cells. A promising route for passivating contacts is their integration into back-contact back-junction (BC-BJ) solar cells indicated by an increase in efficiency of up to 26.1% [9].

As both contacts of BC-BJ solar cells are located at one side of the wafer, the fabrication of such a solar cell requires various patterning steps. Thus, for the formation of local passivating contacts we address printing technology (inkjet- and screen-printing) as an industrially relevant or rather scalable method. The technology of choice would enable a fast and easy fabrication of local passivating contacts and, consequently, an industrially attractive approach for high efficiency and low manufacturing costs.

Inkjet-printing in particular is well suited for BC-BJ solar cells as it allows precise consecutive- or simultaneous local printing of boron- (B) and phosphorus- (P) dopant sources in one printing step [13], which can be combined with one single thermal process step ("co-diffusion") [14]. The appeal of this technology lies in its flexibility, precision, digital printing templates, and the non-contact mode. Because of the latter, wafer breakage and contamination during solar cell manufacturing is reduced, which is important for high efficiency solar cell fabrication.

In this paper, the utilization of printing in order to create local passivating contacts for BC-BJ solar cells is evaluated. The focus is set on inkjet-printing, but in case of B-Doping screen-printing is evaluated, as well. Selected process parameters are tuned in order to achieve adequate quality parameters of recombination and electrical conductivity.

2 EXPERIMENTAL DETAILS

2.1 Lifetime sample preparation

Symmetric lifetime samples were realized on planar shiny-etched (100) oriented phosphorous-doped *n*-type float-zone (FZ) silicon wafers with a specific resistivity of 1 Ωcm and a thickness of 200 µm. To this end, wafers were cleaned according to RCA standard clean procedure and an ultra-thin silicon oxide (SiO_x) layer, approximately 1.3 nm, was thermally grown in a tube furnace at 600°C for 10 minutes on both sides. Subsequently, a 50 nm intrinsic amorphous silicon (a-Si(i)) layer was deposited on both sides of the wafer by LPCVD (deposition temperature of 485°C) (Fig. 1). For reference wafers, B- and P-dopants were introduced into the a-Si(i) layers by ion implantation at ion doses of 1×10^{15} (B) and 2×10^{15} (P) and at ion energy of 2 keV (B) and 5 keV (P) on both sides of the lifetime samples. In order to create dopant sources utilizing printing, B- and P-ink, a *PixDro LP50* inkjet-printer were used. The wafers were dipped in an aqueous solution of 1% hydrofluoric acid (HF) in order to guarantee a clean surface before printing. By a variation of the printing resolution (number of droplets per inch (dpi)) the amount of ink was varied, which results in different thickness values. Each variation was printed on an area of $A = 30 \times 30$ mm^2. After printing, the wafers were cured on a hotplate in order to evaporate the organic components at temperatures of $T_{HP} = 300^oC$ for $t_{HP} = 2$ min (B-ink) and $T_{HP} = 200^oC$ for $t_{HP} = 5$ min (P-ink).

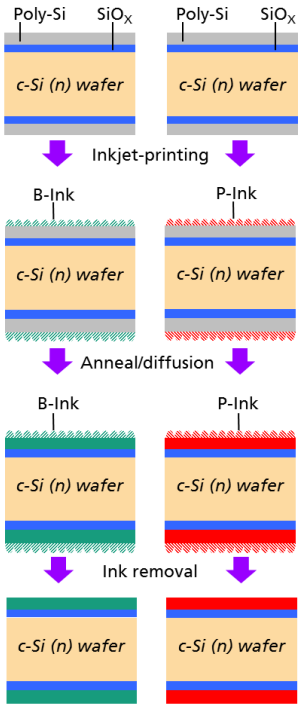

Figure 1: Schematic illustration of the structure of c-Si/SiOx/poly-Si symmetrical lifetime samples. The SiOx layer has been grown thermally in a tube furnace and features a layer thickness of about 1.3 nm. The poly-Si has been deposited by means of LPCVD and features a thickness of 50 nm. The doping of poly-Si layer was realized by inkjet-printing of dopant sources and consequent high temperature anneal.

The curing conditions were determined regarding recommendation of the material suppliers and after performing preliminary experiments. In order to obtain a proper droplet formation and, accordingly, homogeneous layers, the time-dependent piezo-voltage (wave form), firing frequency, or printing resolution were varied. One group of wafers was screen-printed using B-dopant paste. The wafers were subjected to T_{HP} = 400°C on a hotplate for t_{HP} = 3 min.

Afterwards, a high-temperature anneal/diffusion is performed in a tube furnace under nitrogen atmosphere. Four anneal/diffusion profiles were evaluated in these experiments with anneal temperature T_p = 850°C, 900°C or 950°C and annealing time t_p = 10 min or 30 min, as listed in Fig. 2. Following the anneal/diffusion step, residuals were removed in a buffered solution of 1% HF.

2.2 Lifetime sample characterization

After ink/paste removal, the passivation quality on the surface of the symmetrical lifetime samples was measured by means of quasi-steady state photoconductance (QSSPC) measurements through determining implied open-circuit voltage (iV_{OC}) and implied fill factor (i*FF*). These measurements were performed on a WCT-120 lifetime tester from Sinton Instruments [15]. Thereafter, the wafers were subjected to a hydrogenation process in a remote plasma hydrogen passivation (RPHP) system at 400°C for 30 min. The QSSPC measurements were repeated after RPHP in order to investigate the effect of hydrogenation on passivation quality. The sheet resistance of doped regions was

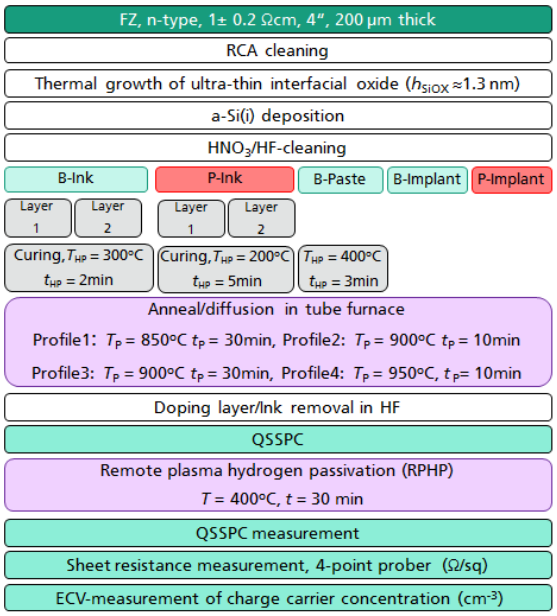

Figure 2: Schematic process sequence for fabrication of lifetime samples. An overview of different groups to investigate influence of the print resolution of the doping layers and the anneal/diffusion plateau time and temperature on passivation quality of layers.

determined by a 4-point prober. Subsequently, the doping profile was measured by electrochemical capacitance voltage (ECV) measurements using a WEP CV21 ECV profiler.

3 RESULTS AND DISCUSSION

3. 1 Inkjet-printing process

In order to optimize the jetting performance for B- and P-inks, the integrated high-speed drop-view camera of the PixDro LP50 was utilized to analyze the droplet formation, while varying the jetting settings. Once an optimal waveform (time-dependent piezo-voltage) for the piezo elements inside the print-head was created, a dynamic droplet analysis (Fig. 3) allows validating that waveform for different nozzles by measuring Volume *V*, velocity *v*, and angle of flying droplets in order to achieve precise printing of droplets onto the silicon substrate. It is clearly visible that the selected nozzles (Fig. 3) are performing similar and enable homogeneous processing. Moreover, undesired defects like the formation of so called satellites, which might induce blurry print products can be avoided. Figure 4 shows a microscopic image of droplets on a textured surface printed by using a 10 pl print-head and a print resolution in x- and y-direction of 100 dpi. The droplet diameter is 108 µm. The vertical and horizontal spacing between droplets (pitch) are 140µm and 134 µm, respectively. These dimensions are very feasible for e.g. consideration within BC-BJ architectures. Further improvements are possible by e.g. utilizing print-heads with lower droplet volume, adapting the waveform, and by heating the substrate during printing. Figure 5 shows a printed layer of B-ink on a shiny-etched FZ substrate with a resolution of 300 × 300 dpi. Different printing parameters were evaluated in order

to achieve complete wafer coverage of the ink, which resulted in formation of two different sizes of droplets.

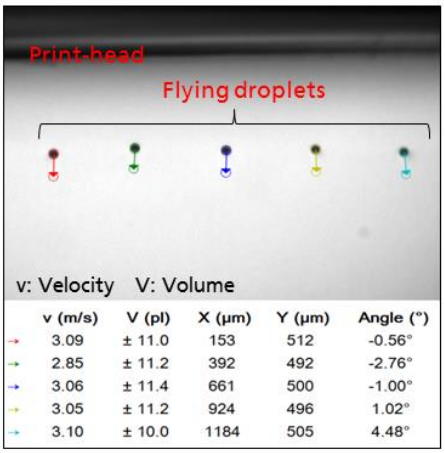

	v (m/s)	V (pl)	X (µm)	Y (µm)	Angle (°)
→	3.09	± 11.0	153	512	-0.56°
→	2.85	± 11.2	392	492	-2.76°
→	3.06	± 11.4	661	500	-1.00°
→	3.05	± 11.2	924	496	1.02°
→	3.10	± 10.0	1184	505	4.48°

Figure 3: Dynamic analysis of the ink-droplets. Volume *V*, velocity *v*, and angle of flying droplets are measured and controlled in order to achieve precise printing of droplets onto the SiO_x-coated Si substrate.

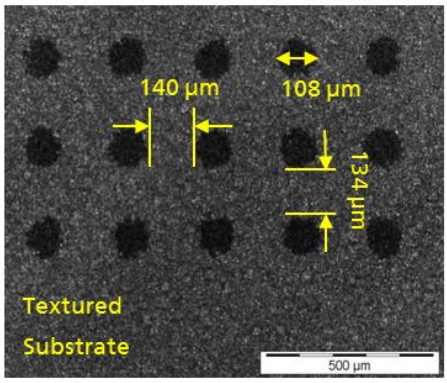

Figure 4: Droplets on a textured surface printed by using a 10 pl print-head and a resolution in x- and y-direction of 100 dpi. Droplet size, vertical and horizontal spacing between lines are illustrated.

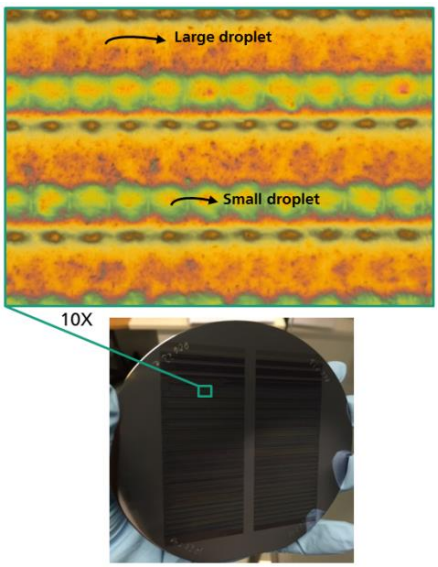

Figure 5: Printed layer on a shiny etched substrate with a resolution of 300 x 300 dpi.

3.2 Passivation quality of lifetime samples

In order to investigate the surface passivation quality, the iV_{OC} and i*FF* values of samples were extracted from injection level dependent lifetime measurements right after the high-temperature anneal/diffusion process (before introducing samples to the RPHP). Considering four different anneal/diffusion processes, the B-ink has an iV_{OC} of around 692 mV being independent of the thermal conditions (Fig. 6(a)), which is similar to the values achieved with the used reference B-ion implantation (Fig. 6 and Table I). In case of B-paste, higher passivation quality of about 700 mV can be achieved at higher diffusion temperatures. The i*FF* of B-ink and B-ion decreases with increasing anneal temperature (Fig. 6(b)). In case of B-paste, a high i*FF* of up to 82.4% can also be achieved at higher diffusion temperatures.

For P-doped samples, the iV_{OC} and i*FF* of P-ink (A) and P-ion improved, respectively, significantly and slightly, by increasing the anneal temperature (Fig. 7(a) and (b)). The improvement resulted in high iV_{OC} and i*FF* for P-ink (A) that is very close to the values of the P-ion reference sample (Table I). After performing RPHP the iV_{OC} of the P-ink (A) improved to 726 mV with an i*FF* = 86.2%, which reveals the excellent passivation quality of the layers. These values are very close to the iV_{OC} = 732 mV and i*FF* = 87.3% obtained from P-ion reference samples after performing RPHP. The P-ink (B) represented a poor passivation quality even at high temperatures. Missing values of iV_{OC} and i*FF* of P-ink (B) at lower temperatures in Fig. 7(a) and (b) are due to the very low carrier's lifetime. In addition of low passivation qualities resulted from P-ink (B), we observed precipitations on the surface of samples after the ink removal step. Table I summarizes the highest iV_{OC} and i*FF* values obtained from each dopant source.

Figure 8(a) shows the phosphorous profiles measured by ECV profiling starting on the poly-Si film and expanded to the c-Si. It can be clearly seen from the profiles that 850°C (30 min) and 900°C (10 min) anneal temperatures are not high enough to enable sufficient diffusion. The abrupt reduction of doping concentration shows the position of the tunnel oxide. The doping profiles were analyzed by EDNA [16]. The sheet resistance of 2.16 kΩ/sq and 1.93 kΩ/sq was calculated, respectively from profiles of samples annealed at 850°C (30 min) and 900°C (10 min). It was observed that by increasing anneal time at 900°C from 10 min to 30 min or increasing the temperature from 900°C to 950°C (10 min), the charge carrier concentration P-ink (A) increases significantly. Specifically, at anneal temperature of 950°C, the surface charge carrier concentration of P-ink (A) is above 10^{20} cm^{-3}, similar to the profile of the P-ion reference sample. The sheet resistance of 272 Ω/sq and 230 Ω/sq were calculated, respectively from P-ink (A) and P-ion profiles. Figure 8(b) illustrates boron profiles measured by ECV profiling. The doping profiles of B-ink samples indicate that an anneal temperature of 950°C leads to excessive diffusion of boron enabling a very deep profile inside c-Si. The calculated sheet resistance of the profile of B-ink samples annealed at 900°C and 950°C are respectively, 228 Ω/sq and 127 Ω/sq. The sheet resistance of the samples measured by a 4-point prober is 306 Ω/sq and 214 Ω/sq, respectively. The calculated sheet resistances are lower than the measured values.

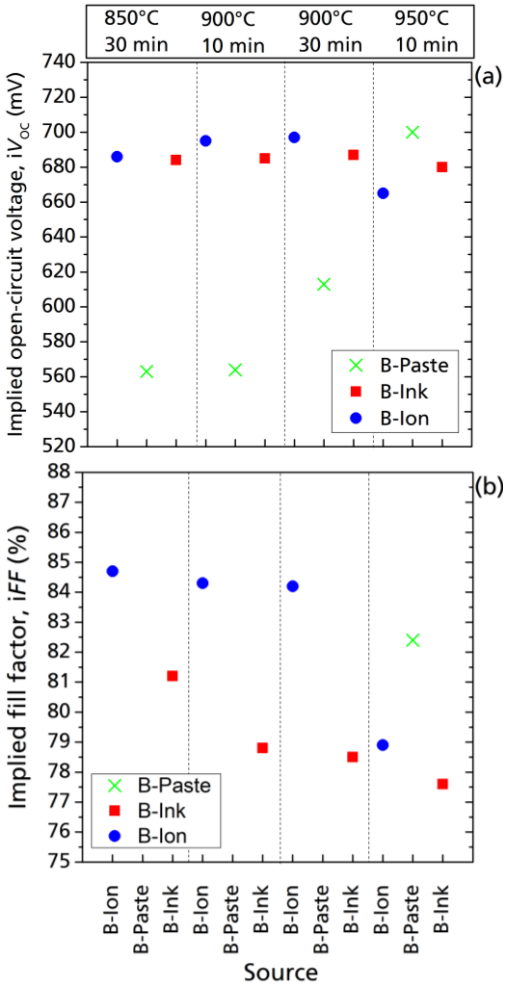

Figure 6: (a) the implied open-circuit voltage (iV_{OC}) and (b) the implied fill factor (i*FF*) vs. boron dopant source for four different diffusion processes, whereas the latter vary in temperature (850°C, 900°C, 950°C) and time (10 min and 30 min).

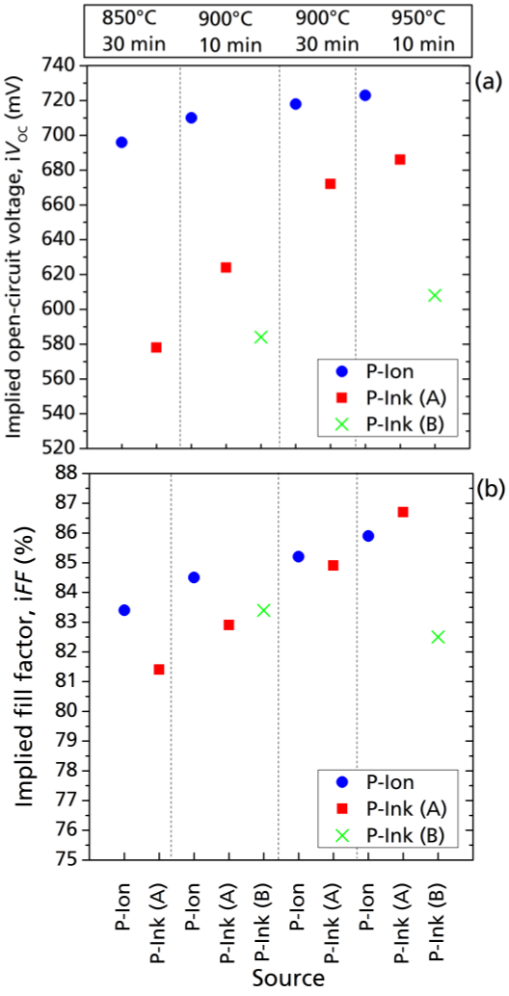

Figure 7: (a) the implied open-circuit voltage (iV_{OC}) and (b) the implied fill factor (i*FF*) vs. phosphorous dopant source for four different diffusion processes, whereas the latter vary in temperature (850°C, 900°C, 950°C) and time (10 min and 30 min).

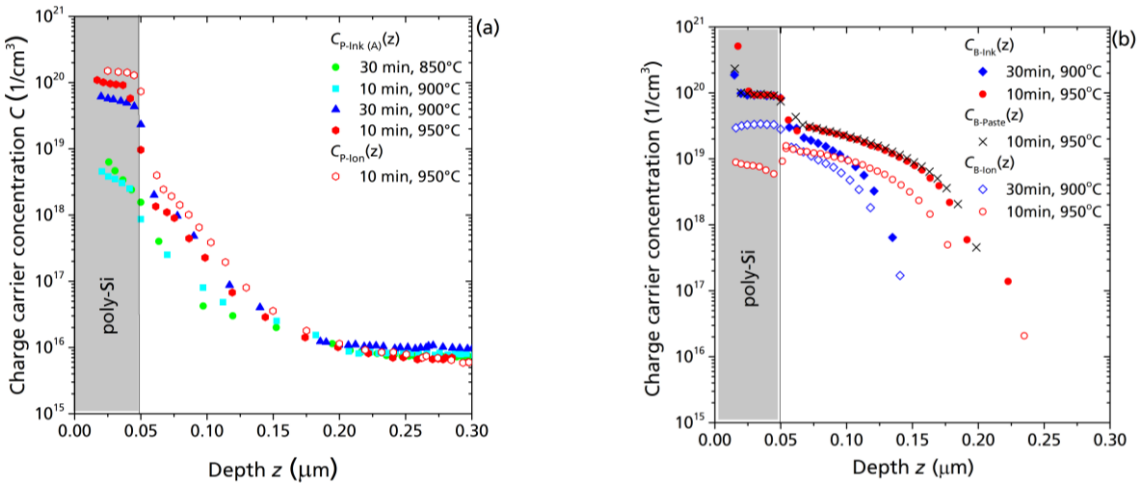

Figure 8: Charge carrier concentration vs. depth for (a) inkjet-printed phosphorus P-Ink (A) and ion-implanted phosphorus P-Ion. (b) inkjet-printed boron B-Ink, ion-implanted boron B-Ion, and screen-printed boron pasteB-Paste.

Table I: Overview of passivating contact's characteristics prepared with inkjet-printed, screen-printed and ion-implanted boron and phosphorous doped poly-Si layers, specifying passivation quality of surfaces before and after applying RPHP (iV_{OC} and i*FF*), the surface charge carrier concentration (C_s), calculated and measured sheet resistances from ECV profiles and by a 4-point prober.

Dopant source	Anneal condition	After Anneal		After H passivation				
		iV_{OC} (mV)	i*FF* (%)	iV_{OC} (mV)	i*FF* (%)	C_s (cm^{-3})	R_{sh} (Ω/sq) from ECV profile	R_{sh} (Ω/sq) from 4pp
P-Ink (A)	950°C, 10 min	686	87.2	726	86.2	10^{20}	272	344
P-Ion (ref)	950°C, 10 min	723	86	732	87.3	10^{20}	230	316
B-Ink	900°C, 30 min	692	82.8	682	80.6	2×10^{20}	228	306
B-Paste	950°C, 10 min	700	82.4	687	83.9	2×10^{20}	170	284
B-Ion (ref)	900°C, 30 min	695	83.2	688	84	2×10^{19}	391	564
B-Ion (ref)	950°C, 10 min	698	84.3	686	83.8	10^{19}	291	515

It is likely because the calculation tool assumes mobility of c-Si for the whole profile, either inside of the poly-Si layer or c-Si. A comparison of the profiles of B-ion and B-ink samples reveals that the amount of surface charge carrier concentration provided by B-ink (>10^{20} cm^{-3}) is much higher than B-ion (~10^{19} cm^{-3}) at the same anneal temperatures.

The B-ion sample annealed at 950°C (10 min) exhibited lower surface charge carrier concentration, but a deeper doping profile inside the c-Si, compared to the B-ion sample annealed at 900°C (30 min). The calculated sheet resistance of profiles is 564 Ω/sq and 515 Ω/sq, respectively. The B-paste sample annealed at 950°C (10 min) showed a similar profile as the B-ink annealed at the same condition. It should be noted that the profiles were measured after applying RPHP.

4 SUMMARY AND CONCLUSION

The poly-Si/SiO_X/c-Si passivating contacts were realized by utilizing inkjet- and screen-printing of phosphorous and boron dopant sources. Inkjet-printed dopant sources could be homogeneously applied with a feature size of around 100µm and a pitch of around 130µm and 140 µm, respectively in x and y direction. The latter are very suitable for integration on Back-Contact Back-Junction silicon solar cells.

The passivation of both inkjet-printed phosphorous and boron doped contacts were studied as a function of anneal/diffusion condition and it turned out that passivation provided by the former was superior to the latter. It was observed that the excellent passivation quality can be achieved by inkjet-printing of phosphorus ink with iV_{OC} = 726 mV and i*FF* = 86.2%. Inkjet-printing of boron ink enables the formation of local passivating contacts with i*V*oc = 692 mV and i*FF* = 82%. The screen-printed boron paste showed a good passivation quality at high annealing temperatures of 950°C with iV_{OC} = 700mV and i*FF* = 82.4%. These results pave the way for future works, where BC-BJ solar cells are fabricated with locally doped *p*- and *n*-type areas, simultaneously applied by inkjet-printing.

Ongoing studies focus on further optimizing printing processes towards higher stability, adapting poly-Si layers for even lower recombination, metallization of doped poly-Si layers and, finally, the preparation of solar cells.

5 ACKNOWLEDGEMENTS

The authors would like to thank anyone involved in this work, the research teams at Fraunhofer ISE PV-TEC and clean room facilities.

This work was supported by the German Federal Ministry for Economic Affairs and Energy within the research project "SiBoKo" under contract number 0324075B and the research project "26+" under the contract number 0325827B.

6 REFERENCES

[1] R. M. Swanson, "Approaching the 29% limit efficiency of silicon solar cells," in *31st IEEE Photovolt. Specialists Conference (IEEEPVSC)*, pp. 889-894, 2005.

[2] A. Richter, M. Hermle, S. W. Glunz, "Reassessment of the limiting efficiency for crystalline silicon solar cells," *IEEE J. Photovolt.*, vol.3, no. 4, pp. 1184-1191, 2013.

[3] F. Feldmann, M. Bivour, C. Reichel, M. Hermle, S. W. Glunz, "A passivated rear contact for high-efficiency n-type silicon solar cells enabling high Vocs and FF > 82%," in *28th European PV Solar Energy Conference and Exhibition (EUPVSEC)*, pp. 988-992, 2013.

[4] F. Feldmann, M. Bivour, C. Reichel, M. Hermle, S.W. Glunz, "Passivated rear contacts for high-efficiency n-type Si solar cells providing high interface passivation quality and excellent transport characteristics," *Sol. Energy Mater. Sol. Cells.*, vol. 120, pp. 270-274, 2014.

[5] F. Feldmann, M. Bivour, C. Reichel, H. Steinkemper, M. Hermle, S.W. Glunz, "Tunnel oxide passivated contacts as an alternative to partial rear contacts," *Sol. Energy Mater. Sol. Cells.*, vol.131, pp. 46-50, 2014.

[6] F. Feldmann, M. Simon, M. Bivour, C. Reichel, M. Hermle, S.W. Glunz, "Efficient carrier-selective p-and n-contacts for Si solar cells," *Sol. Energy Mater. Sol. Cells.*, vol.131, pp. 100-106, 2014.

[7] C. Reichel, F. Feldmann, R. Müller, A. Moldovan, M. Hermle, S. W. Glunz, "Interdigitated back contact silicon solar cells with tunnel oxide passivated contacts formed by ion implantation," in *29th European PV Solar Energy Conference and Exhibition (EUPVSEC)*, pp.487-491, 2014.

[8] D. Yan, A. Cuevas, Y. Wan, J. Bullock, "Passivating contacts for silicon solar cells based on boron-diffused recrystallized amorphous silicon and thin dielectric interlayers," *Sol. Energy Mater. Sol. Cells*, vol. 152, pp. 73-79, 2016.

[9] F. Haase, C. Hollemann, S. Schäfer, A. Merkle, M. Reinäcker, J. Krügener, R. Brendel, R. Peibst, "Laser contact openings for local poly-Si-metal contacts enabling 26.1%-efficient POLO-IBC solar cells," *Sol. Energ. Mat. Sol.*, vol. 186, 2018.

[10] U. Römer, R. Peibst, T. Ohrdes, B. Lim, J. Krügener, T. Wietler, R. Brendel, "Ion implantation for poly-Si passivated back-junction back-contact solar cells," *IEEE J. Photovolt.*, vol.5, pp. 507-514, 2015.

[11] A. Richter, J. Benick, R. Müller, F. Feldmann, C. Reichel, M. Hermle, S. W. Glunz, "Tunnel oxide passivating electron contacts as full-area rear emitter of high-efficiency p-type silicon solar cells," *Progs. Photvoltaics.*, vol. 26, 2017.

[12] M. A. Green, Y. Hishikawa, E. D. Dunlop, D. H. Levi, J. H-Ebinger, A. W. Y. Ho-Baillie, "Solar efficiency tables (version51)," *Prog. Photovolt. Res. Appl.*, vol. 26, 2018.

[13] F. Haase, B. Lim, A. Merkle, T. Dullweber, R. Brendel, C. Günther, M. H. Holthausen, C. Mader, O. Wunnicke, R. Peibst, "Printable liquid silicon for local doping of solar cells," *Sol. Energ. Mat. Sol.*, vol. 179, pp. 129-135, 2018.

[14] R. Keding, D. Stüwe, M. Kamp, C. Reichel, A. Wolf, R. Woehl, D. Borchert, H. Reinecke, and D. Biro, "Co-diffused back-contact back-junction silicon solar cells without gap regions," *IEEE J. Photovolt.*, vol.3, pp. 1236-1242, 2013.

[15] R. A. Sinton, A. Cuevas, "Contactless determination of current-voltage characteristics and minority-carrier lifetime for quasi-steady-state photconductance data," *Appl. Phys. Lett.*, vol. 69, no, 17, pp. 2510-2512, 1996.

[16] K. R. McIntosh, P. P. Altermatt, "A freeware 1D emitter model for silicon solar cells," in *35th IEEE Photovoltaic Specialists Conference (IEEEPVSC)*, pp. 2188, 2010.